Radiative Feedback from Primordial Protostars and Final Mass of the First Stars

Takashi Hosokawa*, Kazuyuki Omukai†, Naoki Yoshida** and Harold W. Yorke*

*Jet Propulsion Laboratory, California Institute of Technology, Pasadena CA 91109, USA
†Department of Physics, Kyoto University, Kyoto 606-8502, Japan
**Kavli Institute for the Physics and Mathematics of the Universe, University of Tokyo, Kashiwa, Chiba 277-8583, Japan

Abstract. In this contribution, we review our efforts toward understanding the typical mass-scale of primordial stars. Our direct numerical simulations show that, in both of Population III.1 and III.2 cases, strong UV stellar radiative feedback terminates mass accretion onto a protostar. An HII region formed around the protostar very dynamically expands throughout the gas accreting envelope, which cuts off the gas supply to a circumstellar disk. The disk is exposed to the stellar UV radiation and loses its mass by photoevaporation. The derived final masses are 43 $M_\odot$ and 17 $M_\odot$ in our fiducial Population III.1 and III.2 cases. Much more massive stars should form in other exceptional conditions. In atomic-cooling halos where H_2 molecules are dissociated, for instance, a protostar grows via very rapid mass accretion with the rates $\dot{M}_* \sim 0.1 - 1\ M_\odot\ \mathrm{yr}^{-1}$. Our new stellar evolution calculations show that the protostar significantly inflates and never contracts to reach the ZAMS stage in this case. Such the "supergiant protostars" have very low UV luminosity, which results in weak radiative feedback against the accretion flow. In the early universe, supermassive stars formed through this process might provide massive seeds of supermassive black holes.

Keywords: cosmology: theory – early universe – stars: formation
PACS: 95.30.Lz, 97.10.Bt, 97.20.Wt

MASS ACCRETION REGULATED BY STELLAR UV FEEDBACK

Population III.1 Stars

The very first stars in the universe (Population III.1 stars) form in massive primordial gas clouds a few hundread million years after the Big Bang. Gravitational collapse of such the cloud gives birth to a tiny ($\sim 0.01\ M_\odot$) embryo protostars surrounded by a massive ($\sim 10^3\ M_\odot$) gas envelope [e.g., 1, 2, 3]. The gas accretes onto the protostar rapidly, which substantially increases the stellar mass [e.g., 4]. The mass of a newly-born star is finally determined when the mass accretion ceases.

It has been predicted that the stellar radiative feedback against the accretion flow could be strong enough to limit the mass accretion [6]. In order to study complex interplay between the stellar radiation and accretion flow, multi-dimensional radiation hydrodynamics simulations following long-term evolution after the birth of the protostar had been awaited. On the other hand, numerical simulations of this sort have been utilized for studying the present-day massive star formation [e.g., 7]. We apply the similar methods to study the primordial star formation [5] (also see H. Susa's and A. Stacy's

© 2012. All rights reserved

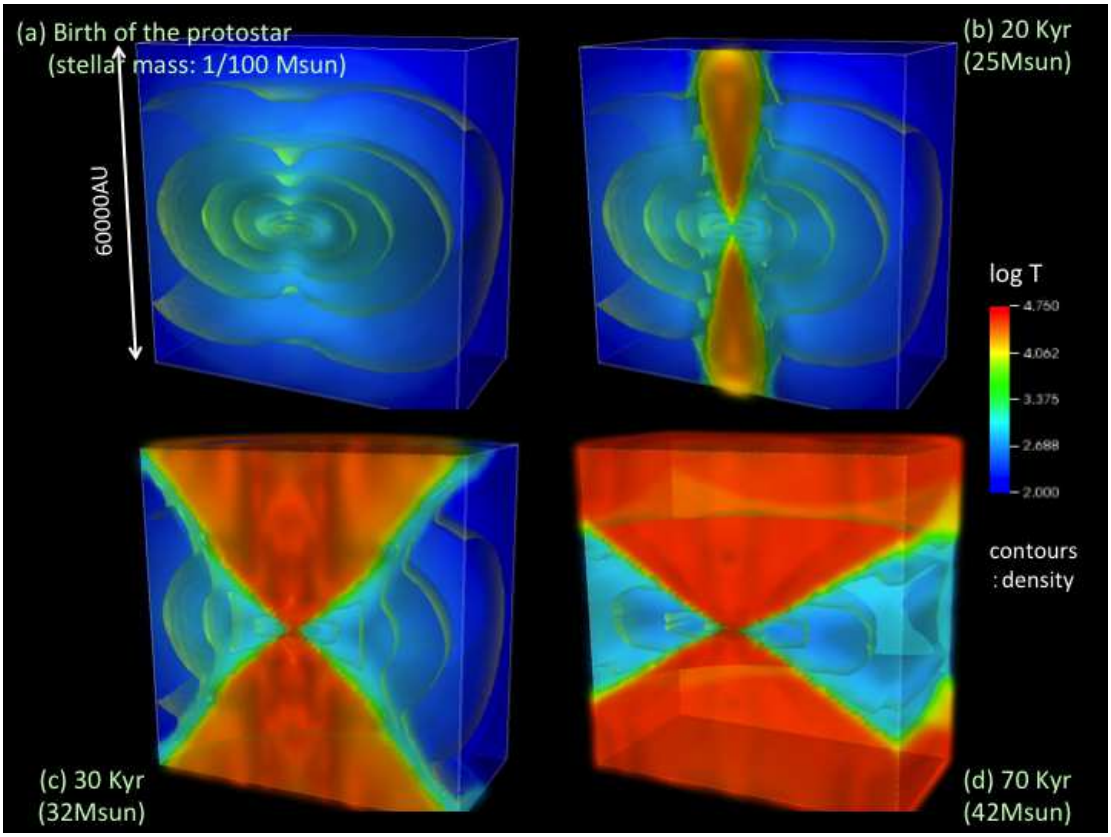

FIGURE 1. Formation and expansion of an HII region around a primordial protostar in the Population III.1 case [5]. The four panels (a) - (d) show the snapshots at the moments of (a) the birth of an embryo protostar ($t = 0$), (b) $t = 2 \times 10^4$ years, (c) 3×10^4 years, and (d) 7×10^5 years. The protostellar masses at these moments are also presented. The colors and contours depict the spatial distributions of the gas temperature and density.

contributions in this volume). We solve the dynamics of the accretion flow employing a 2-dimensional (2D) axisymmetric radiation hydrodynamics code [e.g., 8, 9]. The very vicinity around the protostar is replaced with a sink cell, and mass influx to the sink cell is regarded as the mass accretion rates onto the star. The protostellar evolution is consistently calculated by numerically solving the stellar interior structure with the provided accretion rates [4, 10]. The stellar luminosity and effective temperature, which control the strength of the stellar radiative feedback, are obtained as the results of the stellar evolution calculations. The initial gas distribution is configured with the results of our previous cosmological simulations showing the birth of a Pop III.1 protostar [3].

Figure 1 shows the very dynamical nature of the stellar radiative feedback over $\sim 10^5$ years after the birth of the protostar. We see that the HII region expands throughout the accreting envelope. The circumstellar disk, whose size is $\sim 10^3$ AU from the protostar, lies in the very central part of the presented domain. The mass accretion onto the star is mostly via this accretion disk. As the stellar mass increases, the stellar UV luminosity dramatically rises. The HII region initially grows in the polar directions (Fig.1-b), and then its opening angle increases with the stellar mass (Fig.1-c). High gas pressure within

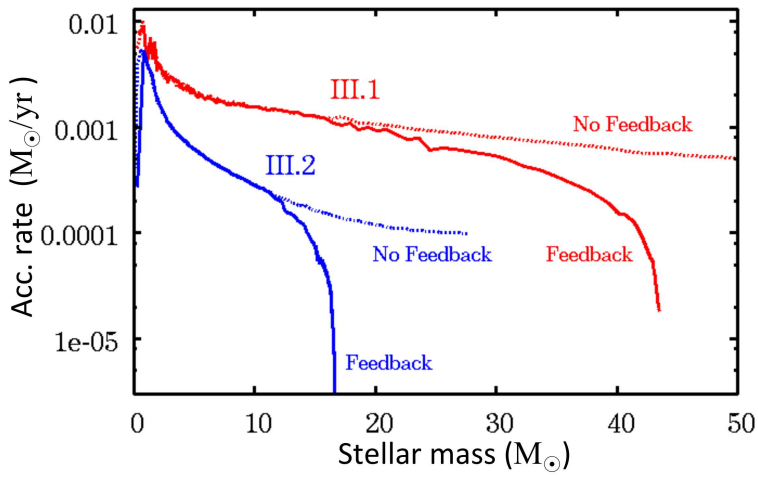

FIGURE 2. Mass accretion histories onto the protostar in our simulations. The red and blue lines represent Population III.1 and III.2 cases. The solid and dotted lines show the evolution calculated with and without radiative feedback.

the HII region drives a shock front going ahead of the ionization front. The shock front propagates throughout the accreting envelope even behind of the circumstellar disk. The shocked materials are pushed away from the star owing to outward pressure gradient, which cuts off the gas supply from the envelope to the disk. The isolated disk is exposed to the stellar UV radiation and being photoevaporated.

Figure 2 shows the mass accretion history onto the protostar during the evolution described above (red solid line). In comparison to the "no feedback" case (red dotted line), we see that the mass accretion rates are reduced by the stellar radiative feedback. The stellar growth in mass is almost terminated at $M_* \simeq 43\ M_\odot$, which suggests that the very first stars should be less massive than previously thought. Such "ordinary" massive stars end their lives as core-collapse supernovae. This explains the fact that any signatures of the pair-instability supernova, which is the final fate of a few $\times 100\ M_\odot$ star, have not been found in the abundance patterns of Galactic metal deficit stars [e.g., 11].

Population III.2 Stars

After the very first stars form, nearby primordial gas could be ionized by their radiative and mechanical feedback. When such the primordial gas recombines and bears the "second-generation" primordial stars, their formation process differs from the Pop III.1 case owing to the enhanced electron abundance (Population III.2 stars). During the early gravitational collapse of a cloud, gas temperature falls down to $\simeq$ a few $\times 10$ K with additional radiative cooling via H_2 and HD molecules [e.g., 12, 13]. The resulting typical mass of the clouds is $\sim$ a few $\times 10\ M_\odot$, which is much lower than in the Pop III.1 case [e.g., 14]. With knowledge of the different mass scales of the cloud, Pop III.1 and III.2 stars had been regarded as the distinct sub-populations which have different stellar

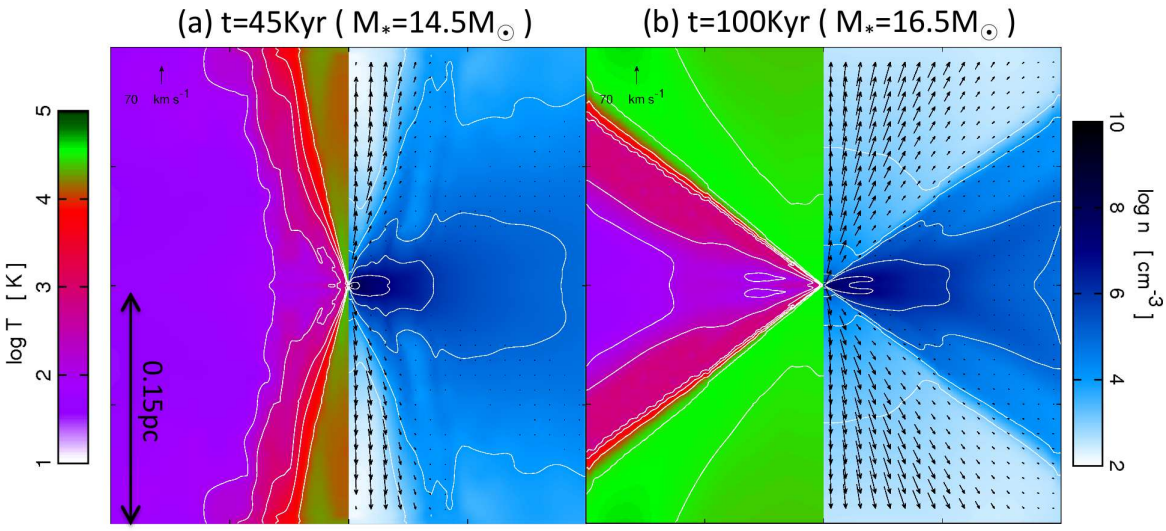

FIGURE 3. Growth of an HII region around the protostar in the Pop III.2 case. The panels (a) and (b) present the snapshots at $t = 4.5 \times 10^4$ years and 10^5 years after the birth of the protostar. The left- and right-hand side of each panel show the spatial distribution of the gas temperature and density. The arrows in the left-hand side represent the distribution of velocity.

masses.

As in the Pop III.1 case, however, the final stellar mass is determined in the later accretion stage. We apply the same numerical method to the Pop III.2 case to follow the long-term evolution until the mass accretion ceases. For the initial gas distribution around the protostar, we again make use of the results of the cosmological simulations following the birth of a Pop III.2 protostar [14].

Figures 2 and 3 show that the strong stellar UV radiative feedback shuts off the mass accretion in the Pop III.2 case as well. However, we also see some quantitative differences between the Pop III.1 and III.2 cases. First, in the Pop III.2 case, the mass accretion rates onto the star are about ten times lower than in the Pop III.1 case (Fig.2). This agrees with the well-known analytic scaling relation $\dot{M}_* \propto T^{3/2}$, where T is the temperature in the gas accreting envelope. With lower accretion rates, in general, the protostar approaches the ZAMS stage for the lower stellar mass [e.g., 4, 10]. The stellar UV luminosity accordingly rises for the lower stellar mass, which explains the lower final stellar mass $M_* \simeq 17\ M_\odot$ in the Pop III.2 case.

Our results suggest that the Pop III.2 stars are less massive than the Pop III.1 stars, but the difference is within a factor of a few. On the other hand, recent 3D numerical simulations are revealing that low-mass ($\sim 1\ M_\odot$) primordial stars could form via gravitational fragmentation of the accretion disk (see T. Greif's and P. Clark's contributions in this volume). However, note that most of such simulations only follow the very early evolution far before the final stellar masses are determined. The stellar radiative feedback should finally limit the mass accretion and set the final stellar mass around tens of solar masses.

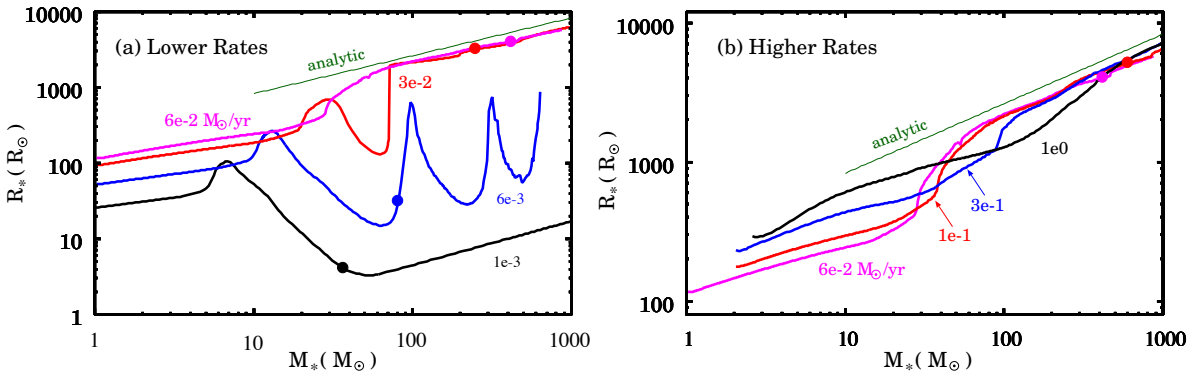

FIGURE 4. Evolution of the protostellar radius with very high accretion rates, (a) $10^{-3}\ M_\odot\ \mathrm{yr}^{-1} \leq \dot{M}_* \leq 6\times10^{-2}\ M_\odot\ \mathrm{yr}^{-1}$, and (b) $6\times10^{-2}\ M_\odot\ \mathrm{yr}^{-1} \leq \dot{M}_* \leq 1\ M_\odot\ \mathrm{yr}^{-1}$ [15]. In each case, the filled circle indicates the epoch when the hydrogen burning begins near the stellar center. The green thin line represents the mass-radius relation given by equation (1).

PROTOSTELLAR EVOLUTION WITH VERY RAPID MASS ACCRETION: EMBRYOS OF SUPERMASSIVE BLACK HOLES?

The above results show that a number of the primordial stars should be ordinary massive stars ($M_* < 100\ M_\odot$). Much more massive stars might form in other exceptional circumstances. Recall that, in the local universe, O-type stars form in such a way, whereas the majority of stars are less massive than $1\ M_\odot$ [7].

In massive dark haloes where H_2 molecules are destroyed by radiative or collisional dissociation [e.g., 16, 17], for instance, a gas cloud nearly isothermally contracts at $T \simeq 8000$ K without strong fragmentation [e.g., 18]. After the birth of a protostar, the stellar mass rapidly increases via mass accretion with very high rates of $\dot{M}_* \sim 0.1-1\ M_\odot\ \mathrm{yr}^{-1}$. If the stellar mass could reach $\sim 10^5\ M_\odot$ by this rapid mass accretion, the star directly collapses to form a massive black hole. The very rapidly accreting protostars could be embryos of supermassive black holes observed in the early universe.

We extend our previous work [4, 10] to study the protostellar evolution in such the extreme situations [15]. We numerically solve the stellar interior structure taking account of the effects of mass accretion. Figure 4 presents the evolution of the stellar radius for $M_* \leq 10^3\ M_\odot$ with various high accretion rates. We see that, with the high accretion rates, the stellar evolution qualitatively differs from the standard one represented for $\dot{M}_* = 10^{-3}\ M_\odot\ \mathrm{yr}^{-1}$. With $\dot{M}_* \geq 6\times10^{-2}\ M_\odot\ \mathrm{yr}^{-1}$, in particular, the stellar radius always increases with the stellar mass. The mass-radius relation for $M_* > 100\ M_\odot$ is almost independent of the different accretion rates. The protostar has the same radius $\simeq 7000\ R_\odot$ ($\simeq 30$ AU) at $M_* = 10^3\ M_\odot$ in the all cases with such high accretion rates.

This unique mass-radius relation of the "supergiant protostars" can be explained with the following simple analytic argument. First, the stellar luminosity is generally written as $L_* = 4\pi\sigma R_*^2 T_{\mathrm{eff}}^4$, where σ is the Stefan-Boltzmann constant. The stellar luminosity is now close to the Eddington value, and the effective temperature is nearly constant at $T_{\mathrm{eff}} \simeq 5000$ K due to the strong temperature-dependence of H^- absorption opacity [19].

With these facts, we obtain

$$R_* \simeq 2.6 \times 10^3\, R_\odot \left(\frac{M_*}{100\, M_\odot} \right)^{1/2}. \tag{1}$$

Figure 4 shows that our numerical results well agree with this relation.

Because of the low effective temperature $T_{\rm eff} \simeq 5000$ K, the UV luminosity of the supergiant protostar is much lower than that of the ordinary Pop III ZAMS stars. Without strong stellar UV feedback, the final stellar mass would be given by the amount of gas which accretes onto the star in its lifetime (also see J. Johnson's contribution in this volume). This could be a formation mode of very massive ($M_* \gg 100\, M_\odot$) stars in the early universe.

ACKNOWLEDGMENTS

T.H. appreciates the support by Fellowship of the Japan Society for the Promotion of Science for Research Abroad. Portions of this work were conducted at the Jet Propulsion Laboratory, California Institute of Technology, operating under a contract with the National Aeronautics and Space Administration (NASA).

REFERENCES

1. K. Omukai, and R. Nishi, *ApJ* **508**, 141–150 (1998).
2. T. Abel, G. L. Bryan, and M. L. Norman, *Science* **295**, 93–98 (2002).
3. N. Yoshida, K. Omukai, and L. Hernquist, *Science* **321**, 669– (2008).
4. K. Omukai, and F. Palla, *ApJ* **589**, 677–687 (2003).
5. T. Hosokawa, K. Omukai, N. Yoshida, and H. W. Yorke, *Science* **334**, 1250– (2011).
6. C. F. McKee, and J. C. Tan, *ApJ* **681**, 771–797 (2008).
7. H. Zinnecker, and H. W. Yorke, *ARA&A* **45**, 481–563 (2007).
8. S. Richling, and H. W. Yorke, *ApJ* **539**, 258–272 (2000).
9. H. W. Yorke, and C. Sonnhalter, *ApJ* **569**, 846–862 (2002).
10. T. Hosokawa, and K. Omukai, *ApJ* **691**, 823–846 (2009).
11. A. Frebel, J. L. Johnson, and V. Bromm, *MNRAS* **392**, L50–L54 (2009).
12. H. Uehara, and S.-i. Inutsuka, *ApJ* **531**, L91–L94 (2000).
13. T. Nagakura, and K. Omukai, *MNRAS* **364**, 1378–1386 (2005).
14. N. Yoshida, K. Omukai, and L. Hernquist, *ApJ* **667**, L117–L120 (2007).
15. T. Hosokawa, K. Omukai, and H. W. Yorke, *ArXiv e-prints* (2012), `1203.2613`.
16. K. Omukai, *ApJ* **546**, 635–651 (2001).
17. K. Inayoshi, and K. Omukai, *MNRAS* **422**, 2539–2546 (2012).
18. V. Bromm, and A. Loeb, *ApJ* **596**, 34–46 (2003).
19. C. Hayashi, *PASJ* **13**, 450–452 (1961).